Supporting Information for

High-yield and high-solubility nitrogen-doped carbon dots: formation, fluorescence mechanism and imaging application

Qian-Qian Shi[a, †], *Yu-Hao Li*[b, †], *Yang Xu*[a], *Yue Wang*[b], *Xue-Bo Yin*[a, *], *Xi-Wen He*[a], *and Yu-Kui Zhang*[a,c]

[a] State Key Laboratory of Medicinal Chemical Biology, Synergetic Innovation Center of Chemical Science and Engineering (Tianjin), and Research Center for Analytical Sciences, College of Chemistry, Nankai University, Tianjin, 300071, China

[b] Key Laboratory of Animal Models and Degenerative Neurological Diseases (Tianjin), School of Medicine, Nankai University, Tianjin, 300071, China

[b] National Chromatographic R. & A. Center, Dalian Institute of Chemical Physics, Chinese Academy of Sciences, Dalian, 116011, China

† These authors contributed equally.

* Corresponding author: Fax: (+86) 22 2350 2458 and E-mail: xbyin@nankai.edu.cn

---

Contents

1. Methods and Materials

1.1 Materials

D-(+)-glucose purchased from Sigma-Aldrich, Shanghai, China. Ethylenediamine tetraaceticacid disodium salt (EDTA), ethanolamine, acetic acid, and ethylenediamine are analytically pure and obtained from the local chemical reagent company.

1.2 Instrumentation

The transmission electron microscopy (TEM) images were performed with Tecnai G^2 F20, FEI Co. (America) operated at an accelerating voltage of 200 kV. The size distribution was measured by calculating more than 200 particles. The infrared spectra were measured by the Bruker TENSOR 27 Fourier Transform Infrared Spectroscopy. The X-ray photoelectron spectroscopy (XPS) analysis was performed by Kratos Axis Ultra DLD spectrometer fitted with a mono chromatic Al K X-ray source (hv 1486.6 eV), hybrid (magnetic/electrostatic) optics, and a multi-channel plate and delay line detector. Both the solid-state and solution-state fluorescence experiments were performed by a Hitachi FL-4500 fluorescence spectrometer. The UV-Vis absorption spectra of C-dots were recorded by a UV-2450-visible spectrophotometer (Shimadzu, Japan) with 1×1 cm quartz cuvette along the 1 cm length. The development of zebrafish fed with C-dots was observed with a fluorescence microscope (Olympus BX51, Japan) equipped with a digital camera.

1.3 Preparation of Nitrogen-doped Cdots (N-Cdots) from EDTA

For the synthesis of N-Cdots, 1.0 g EDTA was dissolved into 10 ml of deionized water followed an ultrasonic treatment to form a colorless solution. The mixture was transferred to a poly(tetrafluoroethylene) Teflon-lined autoclave and heated at 200 °C for 1-12 h. After cooling to room temperature, the homogeneous yellow-brown solution was obtained without apparent sediment. N-Cdots were collected after being filtered with 0.22 μm microporous filter membrane to remove large particles. Finally, the yellow solid of N-Cdots was collected by the vacuum freeze-drying. The N-Cdots are dispersed again from the dry sample for the application.

1.4 Preparation of bare Cdots and passivated N-Cdots

As a comparison, undoped bare Cdots and passivated N-dots were prepared using glucose and EDTA with ethanolamine as precursors, respectively. 120 mg of glucose (0.667 mmole) or 248 mg of EDTA (0.667 mmole) and 200 μL of ethanolamine were dissolved in 10 mL of deionized water, respectively.

Their colorless solutions were added into poly(tetrafluoroethylene) Teflon-lined autoclave and heated at 200 °C for 12 h. The other treatments were in the same way with that for the N-Cdots.

1.5 The *in vivo* fluorescent imaging with the N-Cdots as probe

AB strain zebrafish were used in this study. The animals were maintained in aquaria at 28.5°C with a 10/14-hour dark/light cycle. Embryos were collected after natural spawns, housed at 28.5 °C, and staged by hours post fertilization (hpf). Protocols for all procedures using animals were approved by the Institutional Animal Care Committee at Nankai University. All embryos were grown in 0.003 % 1-phenyl-2-thiourea (PTU, Sigma-Aldrich, St. Louis, MO, USA) to block pigmentation and mediate visualization until 72 hpf. The treated AB strain fertilized embryos were added into 24-well culture plates (8–10 of embryos per well) at 72 hpf. The Cdots were introduced to wells. After cultured for 8 h with tank water containing N-Cdots, zebrafish were treated with free tank water three times to remove excess N-Cdots. The fluorescent images were taken by a Fluorescence microscope (Olympus BX51, Japan) with an excitation of 470–490 nm and emission at 515 nm long passes.

1.6 The biological toxicity study with zebrafish embryos

The 72 hpf zebrafish embryos were added into 24-well culture plates (8–10 of zebrafish embryos per well) and incubated with different concentration of Cdots (0-5 mg mL^{-1}) for 8 hours. The zebrafish was collected to evaluate the *in vivo* biological toxicity of Cdots. All of the experiments were performed under the same conditions for four times, respectively.

1.7 The solid-state fluorescence of the N-Cdots

200 μL of the N-Cdots solution (100 mg mL^{-1}) was cast onto a precleaned microscope slide, with the area 2×2 cm. The slide was covered by dry N-Cdots after vacuum freeze-drying. The solid-state fluorescence was immediately detected to obtain the initial fluorescence value. After that, it was exposed to ambient air under different relative humidity for fluorescence measurement at different period.

1.8 Experiment of Quantum Yields (QY) measure

Quinine sulfate in 0.1 M H_2SO_4 (with the known quantum yield of 0.54 at 360 nm) was chosen as a standard to calculate the quantum yield of Cdots with the following equation:

$$\Phi_x=\Phi_{std}(I_x/I_{std})(\eta^2{}_x/\eta^2{}_{std})(A_{std}/A_x)$$

Where Φ is the quantum yield, I is the measured integrated emission intensity, η is the refractive index, and A is the optical density. The subscript *std* refers to the referenced fluorophore with known

quantum yield. In order to minimize re-absorption effects, absorption was kept below 0.05 at the excitation wavelength of 360 nm.

2. Results and Discussions

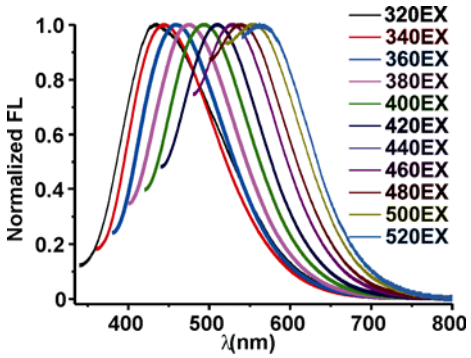

Figure S1. Fluorescence spectra with increasingly longer excitation wavelengths in 20 nm increments with the normalized intensity.

Table S1. Deconvoluted C1s and N1s species, their contents and the Fluorescence spectra at different excitation of the products with different hydrothermal time. (A) 1 h, (B) 4 h, (C) 8 h, and (D) 12 h.

	1 h	4 h	8 h	12 h
C1s	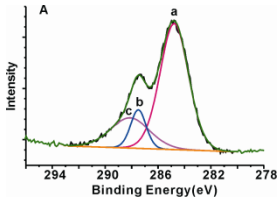	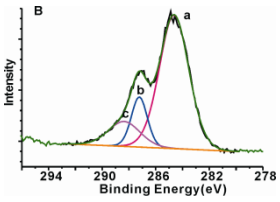	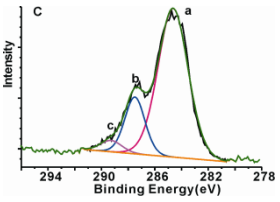	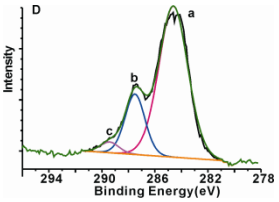
	a. 284.78eV: 66.91%	a. 284.63eV: 71.76%	a. 284.37eV: 76.38%	a. 284.27eV: 75.70%
	b. 287.49eV: 11.12%	b. 287.23eV: 14.51%	b. 287.23eV: 19.46%	b. 287.17eV: 20.84%
	c. 288.12eV: 21.97%	c. 288.36eV: 14.33%	c. 289.01eV: 4.16%	c. 289.08eV: 3.47%
N1s	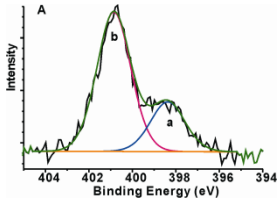	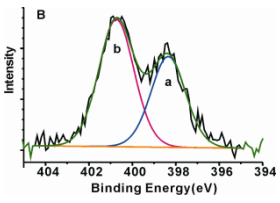	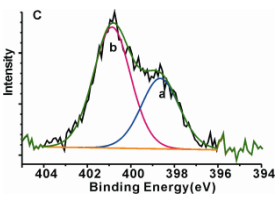	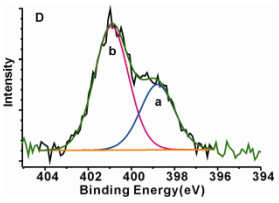
	a. 398.37eV: 27.20%	a. 398.35eV: 40.79%	a. 398.38eV: 37.27%	a. 398.39eV: 36.52%
	b. 400.85eV: 72.80%	b. 400.73eV: 59.21%	b. 400.60eV: 62.73%	b. 400.55eV: 63.48%
FL	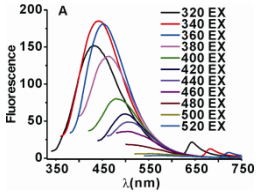	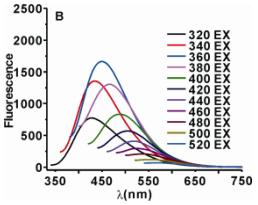	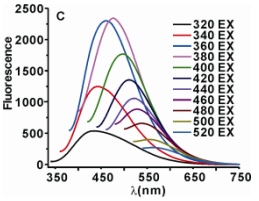	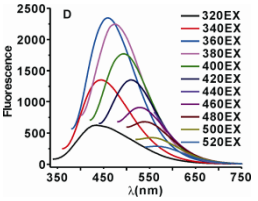

Note. Peaks in C1s spectra are related to the bonds (a) C-C/C=C, (b) C-O/C-N, and (c) C=O; Peaks in N1s spectra are related to the bonds (a) pyridinic N (C-N=C) and (b) graphitic N () or pyrrolic N (C-NH-C); The fluorescence spectra are representative of the original solutions after hydrothermal treatment of EDTA for 1 and 4 h and the 2-fold diluted solutions for 8 and 12 h.

Table S2. Fluorescence quantum yield of r-Cdots and o-Cdots

Sample	*I*	*Abs*	*η*	*QY*
Quinine sulfate	85.90	0.005	1.33	0.54 (known)
N-Cdots	27.85	0.005	1.33	0.175

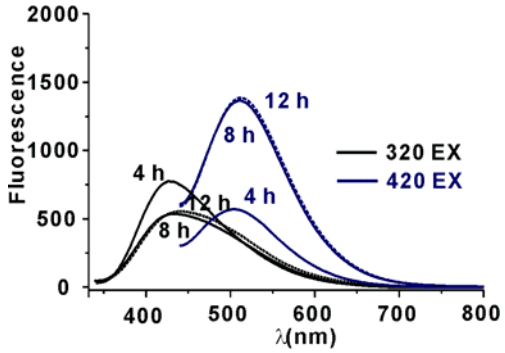

Figure S2. The fluorescence comparison with different incubation time during the preparation procedure at 320 nm and 420 nm excitation. The spectra are obtained from Table 1.

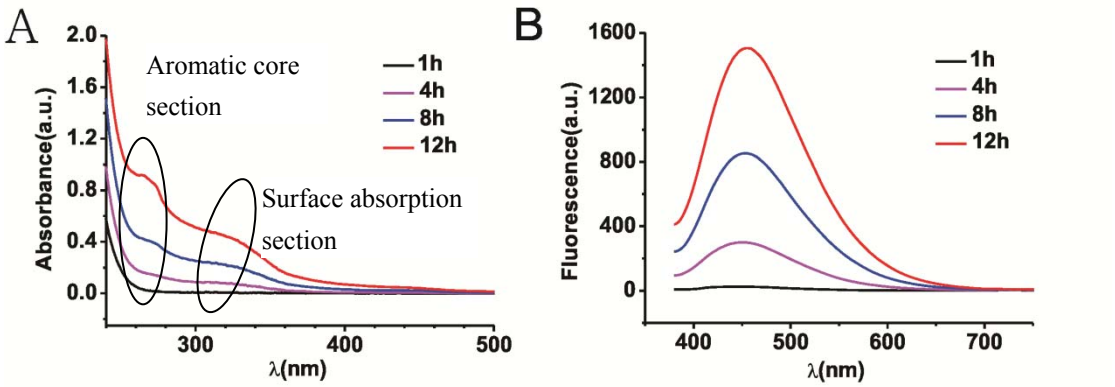

Figure S3. (A) The typical UV and (B) fluorescence spectra of samples after hydrothermal treatment of EDTA with different periods at 360 nm excitation. The 10 times-diluted original solution.

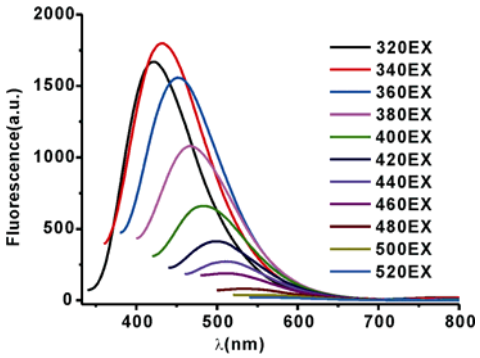

Figure S4. The fluorescence profiles of the products with ethylenediamine and acetic acid (mole ratio 1:4) as precursors after hydrothermal treatment of 8 h.

To validate the formation mechanism of the Cdots through the amido bond, the aqueous solution of ethylenediamine and acetic acid with mole ratio 1:4 was heated at 200 °C for 8 hours. Some nanoparticles were successfully obtained with the same multi-color PL property as the N-Cdots (Figure S4). It provides the possibility to integrate nitrogen into the sketch of carbon network in Cdots with the decomposed products of EDTA.

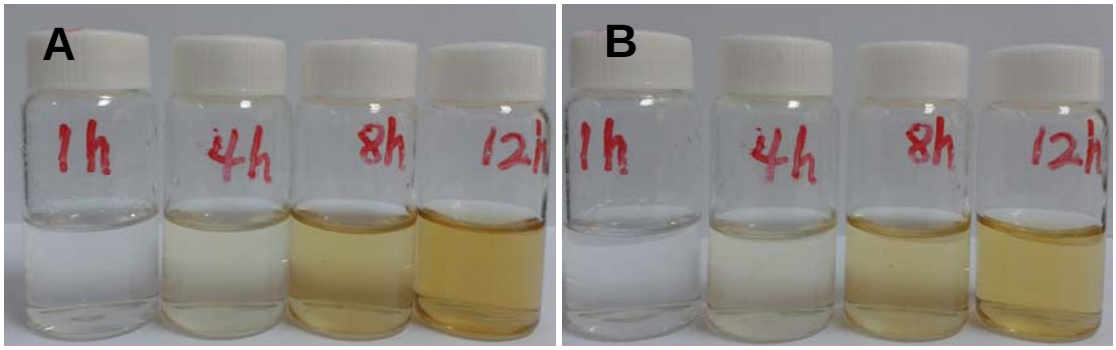

Figure **S5**. The photographs of the products after hydrothermal treatment of EDTA with different time (A) before and (B) after being filtered.

The yield of N-Cdots was calculated to be 78 %, higher than that from the previous Cdots. The crosslinking level and the formation of the product with appropriate size influenced the yield of Cdots. Because the active amine group was the decomposed product from EDTA and the intermolecular amide linkage between the -NH and –COOH groups was limited by the steric hindrance, the condensation polymerization is easily terminated. Therefore, the large carbonized sheet is difficultly formed different to the carbonization procedure of carbohydrate. [1] This was validated by the photos in Figure S4, where the solution is transparent yellow-brown. Almost the same color of the solution before and after filtering

indicates that little participate exists. We have obtained flower-like product for the hydrothermal treatment of EDTA (Figure S6) occasionally; they have the same fluorescence behaviors as the N-Cdots, validating the large carbonized sheet is difficultly formed. Glucose has a high crosslinking level to form large sheet easily for a low Cdots yield. [2] Thus, higher precursor concentration cannot result in a higher harvest of Cdots (Figure S7).[2] Because of the limited condensation polymerization, 100 mg mL^{-1} EDTA can be used as precursor for the improved harvest. Therefore, the alternative advantage of the use of EDTA is the direct formation of N-Cdots with uniform sizes and well monodisperse property because of its limited condensation polymerization. Thus, the procedure is simple and after hydrothermal treatment, only filtering is enough to obtain the N-Cdots.

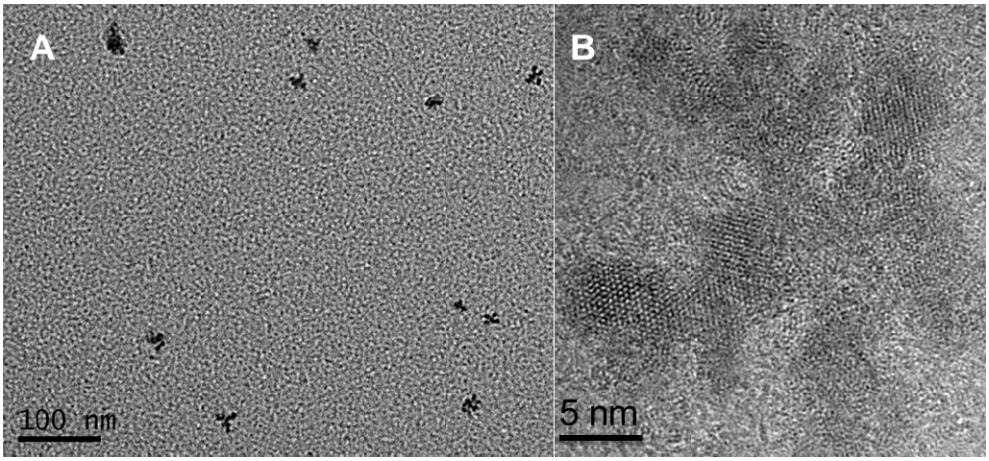

Figure S6. (A) TEM images and (B) the high resolution TEM image of N-Cdots prepared from EDTA.

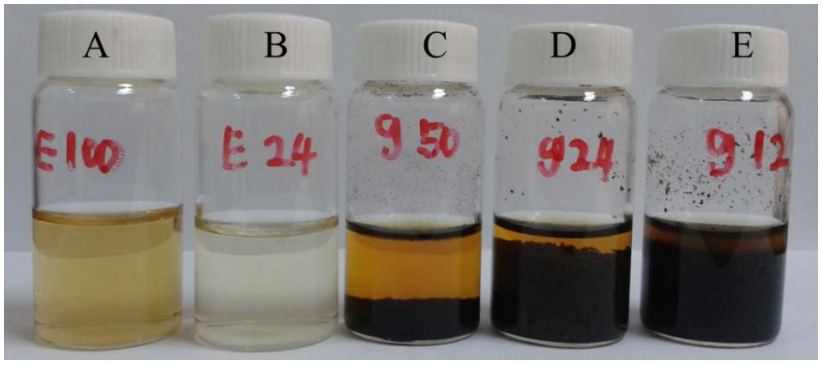

Figure S7. The photos of the products after hydrothermal treatment of (A) 100 mg mL^{-1} EDTA, (B) 24 mg mL^{-1} EDTA, (C) 50 mg mL^{-1} glucose, (D) 24 mg mL^{-1} glucose, and (E) 12 mg mL^{-1} glucose.

Table S3. The yield of carbon dots from previous articles

Method	Carbon precursor	Yield (%)	Ref
Hydrothermal	EDTA	78	This work
Acidic oxidation	Graphene oxide	Not mentioned	3
Acidic oxidation	Carbon black	44.5	4
Acidic oxidation	Activated carbon	>10	5
Hydrothermal	Graphene oxide	5	6
Microwave	Graphene oxide	8	7

The Full References 14

a) K. Howe, M. D. Clark, C. F. Torroja, J. Torrance, C. Berthelot, M. Muffato, J. E. Collins, S. Humphray, K. McLaren, L. Matthews, S. McLaren, I. Sealy, M. Caccamo, C. Churcher, C. Scott, J. C. Barrett, R. Koch, G. J. Rauch, S. White, W. Chow, B. Kilian, L. T. Quintais, J. A. Guerra-Assuncao, Y. Zhou, Y. Gu, J. Yen, J. H. Vogel, T. Eyre, S. Redmond, R. Banerjee, J. Chi, B. Fu, E. Langley, S. F. Maguire, G. K. Laird, D. Lloyd, E. Kenyon, S. Donaldson, H. Sehra, J. Almeida-King, J. Loveland, S. Trevanion, M. Jones, M. Quail, D. Willey, A. Hunt, J. Burton, S. Sims, K. McLay, B. Plumb, J. Davis, C. Clee, K. Oliver, R. Clark, C. Riddle, D. Eliott, G. Threadgold, G. Harden, D. Ware, B. Mortimer, G. Kerry, P. Heath, B. Phillimore, A. Tracey, N. Corby, M. Dunn, C. Johnson, J. Wood, S. Clark, S. Pelan, G. Griffiths, M. Smith, R. Glithero, P. Howden, N. Barker, C. Stevens, J. Harley, K. Holt, G. Panagiotidis, J. Lovell, H. Beasley, C. Henderson, D. Gordon, K. Auger, D. Wright, J. Collins, C. Raisen, L. Dyer, K. Leung, L. Robertson, K. Ambridge, D. Leongamornlert, S. McGuire, R. Gilderthorp, C. Griffiths, D. Manthravadi, S. Nichol, G. Barker, S. Whitehead, M. Kay, et al., *Nature* **2013**, *496*, 498-503; b) R. N. Kettleborough, E. M. Busch-Nentwich, S. A. Harvey, C. M. Dooley, E. de Bruijn, F. van Eeden, I. Sealy, R. J. White, C. Herd, I. J. Nijman, F. Fenyes, S. Mehroke, C. Scahill, R. Gibbons, N. Wali, S. Carruthers, A. Hall, J. Yen, E. Cuppen, D. L. Stemple, *Nature* **2013**, *496*, 494-499.

3. Supplementary References

1. X. Sun, Y. Li, *Angew. Chem. Int. Ed.* **2004**, *43*, 597-601.
2. Z.-C. Yang, X. Li, J. Wang, *Carbon* **2011**, *49*, 5207-5212.
3. J. Shen, Y. Zhu, X. Yang, J. Zong, J. Zhang and C. Li, *New J Chem*, 2012, **36**, 97-101.
4. Y. Dong, C. Chen, X. Zheng, L. Gao, Z. Cui, H. Yang, C. Guo, Y. Chi and C. M. Li, *J Mater Chem*, 2012, **22**, 8764-8766.
5. Y. Dong, N. Zhou, X. Lin, J. Lin, Y. Chi and G. Chen, *Chem Mater*, 2010, **22**, 5895-5899.
6. D. Pan, J. Zhang, Z. Li and M. Wu, *Adv Mater*, 2010, **22**, 734-738.
7. L.-L. Li, J. Ji, R. Fei, C.-Z. Wang, Q. Lu, J.-R. Zhang, L.-P. Jiang and J.-J. Zhu, *Adv Funct Mater*, 2012, **22**, 2971-2979.